20. Hsiung, J. & Newell, R. E. *J. phys. Oceanogr.* **13**, 1957-1967 (1983).
21. Paltridge, G. & Woodruff, S. *Mon. Weath. Rev. U.S Dep. Agric.* **112**, 1093-1095 (1984).
22. Douglas, A., Cayan, D. & Namias, J. *Mon. Weath. Rev.* U.S. Dep. Agric. **110**, 1851-1862 (1982).
23. Cadet, D. L. & Diehl, B. C. *Mon. Weath. Rev.* U.S. Dep. Agric. **112**, 1921-1935 (1984).
24. Barnett, T. P. *Mon. Weath. Rev. U.S. Dep. Agric.* **112**, 303-312 (1984).
25. Oort, A. H. & Maher, M. C. in *Coupled Ocean-Atmosphere Models* (ed. Nihoul, J.) 183-198 (Elsevier, Amsterdam, 1985).
26. Rind, D. & Rossow, W. B. *J. atmos. Sci.* **41**, 479-507 (1984).
27. Gadgil, S., Joseph, P. V. & Joshi, N. V. *Nature* **312**, 141-143 (1984).
28. Palmer, T. N. and Mansfield, D. A. *Q. J. R. met. Soc.* (in the press).
29. Jaeger, L. *Berichte Deutscherwetterd* Vol. 18, No. 139 (1976).
30. Palmer, T. N. *Nature* (in the press).

Glaciers as indicators of a carbon dioxide warming

J. Oerlemans

Institute of Meteorology and Oceanography, University of Utrecht, Princetonplein 5, Utrecht, The Netherlands

During the past 150 years, mountain glaciers have shown a worldwide retreat. It has been argued that this is related to the warming which is predicted to result from increased carbon dioxide levels in the atmosphere; however, this warming has not been detected in a statistically significant way from instrumental records. I demonstrate here that the lower part of a valley glacier is extremely sensitive to a local warming, induced by an increase in the radiation budget. For glaciers covering only a small fraction of a valley, the effect is particularly dramatic. Thus valley glaciers may be extremely vulnerable to the presence of infrared-absorbing gases in the atmosphere, and could therefore be better detectors of a possible carbon dioxide warming than is generally assumed.

Climatic indicators such as tree-ring width, sea level and glacier variations can extend our knowledge of the Earth's climatic history beyond the relatively recent period covered by instrumental records. In Europe, the presence of long valley glaciers in areas that have been populated for hundreds of years provides long records of glacier front variations. Figure 1 shows records of three glaciers in the Alps and one in Norway (Nigardsbreen)[1-5]. The dramatic retreat of these large glaciers since 1850 is generally believed to be part of a worldwide retreat, which contributed significantly to the observed rise in global sea level[6]. It is therefore natural to ask whether our knowledge of historic glacier variations can be of some value with regard to the carbon dioxide issue.

Many factors affect the annual mass balance of a glacier[7-10]; depending on type of glacier and climatic conditions, these include winter accumulation, summer temperature, cloudiness and early summer snowfall. Here I concentrate on melting rates at the lower parts of long glaciers, such as those referred to in Fig. 1. Such glaciers have their snout at altitudes where mean air temperature is far above the melting point in summer, and advective transfer of heat from regions surrounding the glacier is a very important factor. As will be demonstrated, this advective transfer amplifies the sensitivity of melting rates to changes in the radiation budget.

The calculation described below is based on a highly simplified model of the energy budget of a valley-glacier system, in which a daily cycle is obtained for four dependent variables; namely, surface temperature of the glacier (θ_s), surface temperature of the surrounding regions (T_s), mean boundary-layer temperature over the glacier (θ_a) and mean boundary-layer temperature over the surrounding regions (T_a). Here, the surface temperature is the mean temperature of the surface layer involved in the daily cycle, and the boundary-layer temperature is the mean air temperature in the lowest 1-1.5 km of the atmosphere.

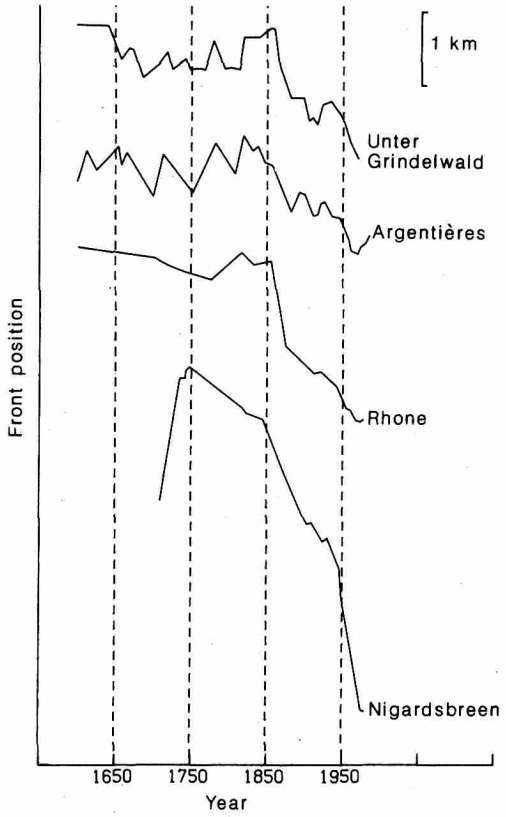

Fig. 1 Front variations of three valley glaciers in the Alps and one in Norway (Nigardsbreen). Data from refs 1-5. The retreat since 1850 is striking.

A diagram of the model is shown in Fig. 2. There are four boxes which interact by radiative processes (single arrows) and by turbulent and advective heat fluxes (double arrows). The surface layers also lose energy to space: a small part of the outgoing infrared flux escapes directly. The background atmosphere has a prescribed characteristic temperature T_b, so the radiation balance of this layer is irrelevant. Absorption of solar radiation in the boundary layer is ignored, so the model is forced by the absorption of solar energy at the surface.

The boundary is assumed to have an effective long-wavelength emissivity μ, while that of the background atmosphere is denoted by ν. The radiation balance of the surface layer (surrounding ground) can then be formulated as:

$$R_s = AQ(t) - \sigma T_s^4 + \mu\sigma T_a^4 + (1-\mu)\nu\sigma T_b^4, \qquad (1)$$

and the expression for the boundary layer is:

$$R_a = \mu\sigma T_s^4 - 2\mu\sigma T_a^4 + \mu\nu\sigma T_b^4 \qquad (2)$$

In equation (1), the first term on the right-hand side represents the absorption of solar radiation at the surface (Q is incident radiation, A effective absorptivity), the second term the upward long-wavelength emission, and the third and fourth terms counter-radiation from the atmosphere. σ is the Stefan-Boltzmann constant. The interpretation of equation (2) is similar, but there is no short-wavelength (solar) contribution. Equivalent equations can be written for the glacier, but the absorptivity will generally be lower.

A few comments on the effective absorptivity A are in order. In the present schematic calculation, effects such as those of cloud cover and atmospheric dust content are all absorbed in this quantity. A simply indicates what fraction of the solar radiation incident at the top of the atmosphere is absorbed at the surface. This implies that in the sensitivity experiments

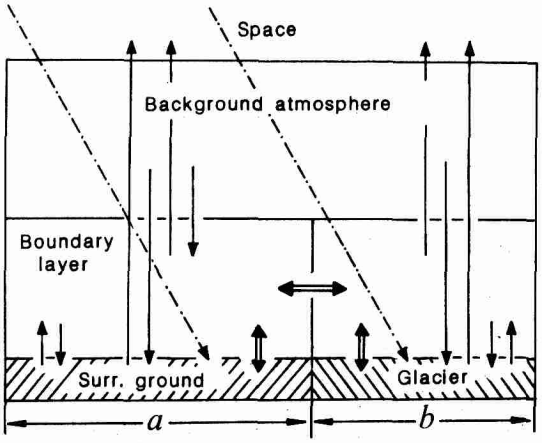

Fig. 2 Schematic representation of the energy fluxes included in the model calculation. The geometry is characterized by length scales a (surrounding ground) and b (glacier). Single arrows, radiative fluxes (solid lines, long-wavelength; broken line, solar). Double arrows, tubulent and advective heat fluxes.

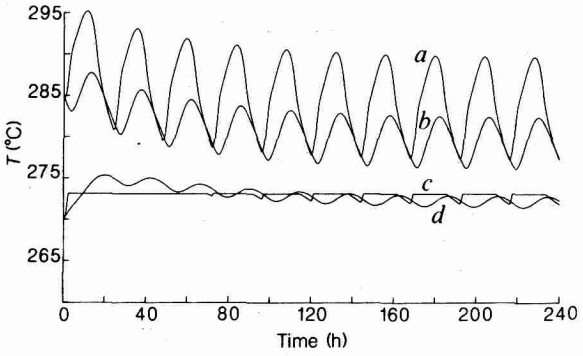

Fig. 3 Standard run showing how the system settles to stationary conditions. The curves are: a, surface temperature of the surrounding ground; b, mean boundary-layer temperature over the surrounding ground; c, surface temperature of the glacier tongue; d, mean boundary-layer temperature over the glacier. For this particular run, model parameters are: $\mu = 0.3$, $\nu = 0.8$, $T_b = 245$ K, $C = 10^6$ J m^{-2} K^{-1}, surface-layer heat capacity $= 3 \times 10^5$ J m^{-2} K^{-1}, $D = 10$ m^2 s^{-1}, $a = 5{,}000$ m and $b = 1{,}000$ m. These estimates were derived from standard physical climatology[13].

discussed below, all factors determining the effective absorptivity remain unchanged.

Turbulent heat fluxes occur between surface layer and boundary layer (vertical fluxes) and advective heat transport between glacier and surroundings in the boundary layer (horizontal fluxes). The vertical fluxes are set proportional to the difference in potential temperature. The exchange coefficient also depends on this difference, because the suppression of heat fluxes in a stably stratified atmosphere is an important feature even for the present schematic model. The dependence on stratification was formulated in agreement with current ideas[11]. With regard to the daily cycle in fairly stable conditions (which is of interest here), inclusion of an advective heat flux between boundary layer and background atmosphere did not result in significant effects, so it is neglected here.

When considering horizontal energy fluxes, geometric effects come into play more explicitly. If the glacier and the surrounding area are characterized by length scales b and a, respectively, then the quantity $b/(a+b)$ gives the fraction of a valley covered by glacier ice. In a first-order approximation it is reasonable to set the horizontal energy transport proportional to the boundary-layer temperature difference over the glacier and the surrounding regions. The rate equations for T_a and θ_a are then of the form:

$$\frac{dT_a}{dt} = R_a/C - k(T'_a - T_s) - (T_a - \theta_a)D/[a(a+b)] \quad (3)$$

$$\frac{d\theta_a}{dt} = P_a/C - k(\theta'_a - \theta_s) - (\theta_a - T_a)D/[b(a+b)] \quad (4)$$

The prime indicates potential temperature, P_a is the radiation balance of the boundary layer over the glacier, C is the heat capacity of the boundary layer (per unit area), k the vertical and D the horizontal exchange coefficient.

The model is completed by similar rate equations for T_s and θ_s, details of which will not be given here. An additional condition is that θ_s cannot exceed the melting point. When the glacier surface is at the melting point all surplus energy is used for melting.

The system of four coupled equations is easily solved on a computer. An example is shown in Fig. 3; model parameters are given in the legend. The forcing function $Q(t)$ consists of half of a sine function in time (half-period 16 h), with a peak value of 700 W m^{-2}. The effective absorptivity is set to 0.5 over the glacier and to 0.75 over the surrounding region.

After about 5 days of integrated time the model temperatures settle to a steady regime. The amplitudes of the daily variation are quite reasonable, as are the observed phase shifts. T_s an θ_s are almost in phase with $Q(t)$ (not shown). The boundar layer temperature over the glacier (curve d) shows the large shift: it reaches a maximum value in the beginning of the evenin This result is difficult to verify from existing observations, b it is probably correct. The amount of melt water produced i the last cycle of this run corresponds to 0.0622 m ice per da

Calculated melt rates are particularly sensitive to the atmo pheric background temperature (T_b) and to the horizont energy fluxes. Changing T_b by 5 K leads to a change of 2 cm i daily melt. Reducing D by 50% cases a 35% decrease in dai melt, doubling D a 30% increase. This demonstrates that muc of the energy used for melting is imported from the regio surrounding the glacier tongue.

A series of model runs was carried out to investigate th sensitivity of the melting rates to changes in the radiation ba ance. One can think of sophisticated ways to mimic the effe of an increasing carbon dioxide concentration in the atmo phere, but here I simply assume that the radiation balance the surface is perturbed by a constant value of 6 W m^{-2}. Suc a value is mentioned in the literature as characteristic of doubling of the carbon dioxide concentration[12]. For each several sets of model parameters, the following runs were carrie out: (1) radiation perturbation over the glacier only, (2) radiatio

Table 1 Melt rates (mm ice per day) obtained in sensitivity tests

Run	(a, b) (m) (5,000, 5,000)	(5,000, 2,000)	(5,000, 1,000)	(5,000, 500)	(1,000, 200
Standard	5.45	23.1	62.2	117	134
(1)	6.83	24.8	63.6	118	135
(2)	7.31	27.0	70.6	130	148
(3)	8.56	30.1	76.9	139	158

The standard run corresponds to the case shown in Fig. 3, for various valu of the length scales a and b. Run (1), the radiation input to the glacier surface increased by 6 W m^{-2}; run (2), the radiation input to the entire region is increas by this amount; run (3), as for run (2), with an additional increase of 1.5 K the atmospheric background temperature T_b.

perturbation over the entire region, and (3) as in the previo experiment with an additional increase in T_b of 1.5 K.

The results are shown in Table 1. Those in the top ro correspond to the standard case of Fig. 3. If the glacier receiv an additional 6 W m^{-2}, this leads to an increase in daily me of 1.4 mm ice. If the entire region has an increased radiatic balance, this value increases to 7.1 mm. An additional increa of 1.5 K in T_b would bring the total increase of melt to 14.7 mr

The effect on melting rates of increasing energy transport to the glacier is largest when the glacier occupies a relatively small area, as is the case for a swiftly retreating glacier tongue.

This sensitivity experiment clearly demonstrates that a glacier can make use of surplus radiation in a valley in a very efficient way. The fact that the surface temperature of the glacier cannot rise above the melting point is crucial. Any increase in radiation thus causes an increased temperature difference between glacier and surrounding regions and thus a larger horizontal energy transfer. This 'oasis effect' disappears when a region becomes completely glaciated.

The glacier may respond in a similar fashion to changes in the background climatic state, which is represented in the present simple model by T_b. The third run, in which an increase in T_b is included, was carried out with this in mind. Even when this effect is not included, melting rates on a small glacier tongue may increase by as much as 15% for a 6 W m^{-2} increase in the radiation input. Through the mechanism discussed here, the glacier retreat establishes a positive feedback. A retreat of the glacier front is associated with decreasing ice thickness and hence with decreasing width of the glacier. In terms of the present model, b thus increases and a further change in melt rate will result. This process can be particularly effective when bare rock is involved.

In this simple calculation I have considered only one of many processes which determine the response of mountain glaciers to rising carbon dioxide levels in the atmosphere. Changes in atmospheric circulation will lead to changes in the amount of cloud cover and precipitation (snow cover in spring could be particularly important[14]). Nevertheless, the direct effect of a change in radiation on melting rates at the glacier tongue would seem to be most important.

Given that the timescale of front variations associated with changes in melt rates at the tongue is very short (of the order of decades), the observed glacial retreat can well be explained by the increasing carbon dioxide level in the atmosphere. Due to the oasis effect, valley glaciers can be considered as very good indicators of climatic change induced by small shifts in the long-term radiation balance.

This research is sponsored by the Ministry of Housing, Physical Planning and Environment (The Netherlands) under contract 611003.01.

Received 5 November 1985; accepted 12 February 1986.

1. Messerli, B., Messerli, P., Pfister, C. & Zumbühl, H. J. *Arct. alp. Res.* **10**, 247-260 (1978).
2. Vivian, R. *Les Glaciers des Alpes Occidentales* (Allier, Grenoble, 1975).
3. Messerli, B. *et al. Z. Gletscherk. Glazialgeol.* **9**, 3-110 (1975).
4. International Association of Scientific Hydrology *Fluctuations of Glaciers* Vols 1-3 (UNESCO, Paris, 1967, 1973, 1977).
5. Ostrem, G., Liestol, O. & Wold, B. *Norsk geogr. Tidsskr.* **30**, 187-209 (1977).
6. Meier, M. F. *Scieence* **226**, 1418-1421 (1984).
7. Martin, S. *Z. Gletscherk. Glazialgeol.* **13**, 127-153 (1977).
8. Young, G. J. *Z. Gletscherk. Glazialgeol.* **13**, 111-125 (1977).
9. Reynand, L. in *Varuations in the Global Water Budget*, (eds?) 197-205 (Reidel, Dordrecht, 1983).
10. Kuhn, M. in *Sea Level, Ice and Climatic Change* (ed. Allison, I.) 3-20 (International Association of Scientific Hydrology, Paris, 1979).
11. Louis, J. F. *European Centre for Medium Range Weather Forecasts intern. Rep.* no. 4 (Reading, 1977).
12. Ramanathan, V. *J. atmos. Sci.* **38**, 918-930 (1981).
13. Sellers, W. D. *Physical Climatology* (University of Chicago Press, 1965).
14. Kukla, G. in *Sea Level, Ice and Climatic Change* (ed. Allison, I.) International Association of Scientific Hydrology, 79-108 (UNESCO, Paris, 1979).